Host–guest coupling in semiconducting $Ba_8Zn_8Ge_{38}$

2008 J. Phys.: Condens. Matter 20 104244

(http://iopscience.iop.org/0953-8984/20/10/104244)

IOP Publishing Journal of Physics: Condensed Matter

J. Phys.: Condens. Matter **20** (2008) 104244 (6pp) doi:10.1088/0953-8984/20/10/104244

Host–guest coupling in semiconducting $Ba_8Zn_8Ge_{38}$

M Christensen[1] **and B B Iversen**[2]

Department of Chemistry, University of Aarhus, DK-8000 Århus C, Denmark

E-mail: bo@chem.au.dk

Received 9 July 2007, in final form 12 September 2007
Published 19 February 2008
Online at stacks.iop.org/JPhysCM/20/104244

Abstract

Two samples of the type I clathrate $Ba_8Zn_8Ge_{38}$ have been prepared by a self-flux method with different cooling rates. Transport properties have been measured for a large single crystal of $Ba_8Zn_8Ge_{38}$ from the slow cooled batch, and they reveal the sample to be semiconducting. A high Seebeck coefficient of $-175\ \mu V\ K^{-1}$ was observed at 400 K. High resolution single crystal neutron diffraction data measured for both slow cooled and fast cooled samples reveal significant differences in the guest atom nuclear density, which can be related to the occupancies of Zn in the host structure framework. Analysis of the atomic displacement parameters shows that the Einstein temperatures of the barium guest atoms are of comparable size at 62 and 67 K for the slow and fast cooled samples, respectively. The Debye temperature for the host framework was in both cases found to be ∼280 K.

(Some figures in this article are in colour only in the electronic version)

1. Introduction

The interest in inorganic clathrates has flourished in recent years, mainly due to the potential application of clathrates in thermoelectric power generators. A thermoelectric module placed in a temperature gradient causes the electrons or holes from the hot side to migrate to the cold side producing a voltage difference. Phonons also carry heat, but they do so without producing a voltage difference. Therefore, the thermal conductivity associated with the phonon drift needs to be minimized. A dimensionless thermoelectric figure of merit can be defined as $zT = TS^2\sigma/(\kappa_L + \kappa_e)$, where T is the temperature, S the Seebeck coefficient, σ the electrical conductivity, κ_e the thermal conductivity associated with the charge carriers and κ_L the phonon contribution to the thermal conductivity.

The exceptional property of the clathrates is low lattice thermal conductivity. Despite high crystallinity clathrates conduct heat like a glass. The low thermal conductivity partly originates from loosely bound guest atoms residing in oversized cages formed by the host structure atoms. The type I clathrate has a cubic structure belonging to space group $Pm\bar{3}n$. It contains two differently sized cages, and the centers of the cages are denoted 2a and 6d, respectively. The host structure has three unique sites denoted 6c, 16i and 24k. Figure 1 shows a part of the unit cell with emphasis on the cage structure

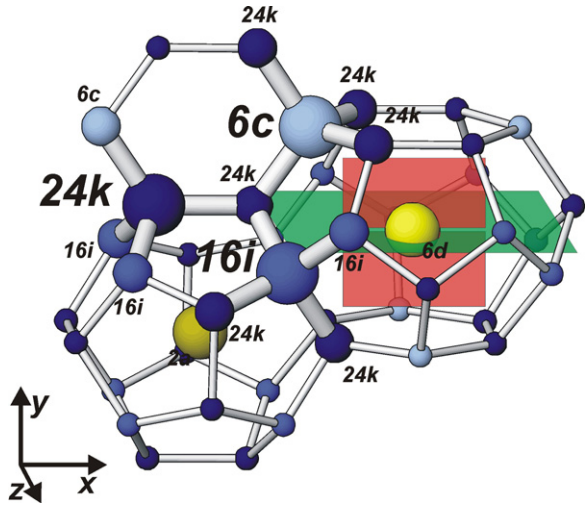

Figure 1. The clathrate type I structure with emphasis on the two cages. The planes in the large cage correspond to the equatorial plane and the perpendicular plane. The shading of the host structure atoms refers their siting, 6c (light) 16i (medium) and 24k (dark). The bonding arrangement around the different host structure atoms has been emphasized by varying the radius of the spheres.

[1] Present address: Bragg Institute, ANSTO, Lucas Heights, NSW 2234, Australia.

[2] Author to whom any correspondence should be addressed.

and the bonding environment. The Zintl concept provides a guideline for determining the stoichiometry of the type I clathrates. The ionic guest atoms donate valence electrons to the host structure, which form the tetrahedrally coordinated covalent framework. According to the Zintl concept the clathrates should be semiconducting compounds at a valence electron count of 184, but in fact the majority of clathrates reported in the literature reveal metallic behavior [1–4]. This also holds true for earlier studies on samples with reported ideal stoichiometry $Ba_8Zn_8Ge_{38}$ [5, 6].

In the literature most attention has focused on the guest atoms, whereas less attention has been paid to the host structure. This is presumably because it is difficult to distinguish neighboring element in the host structure using x-ray diffraction. This is particularly the case for some of the best known clathrates; $X_8Ga_{16}Ge_{30}$ (X = Eu, Sr, and Ba) [2, 7–11], $X_8Zn_8Ge_{38}$ (X = Sr, Ba) [5, 6, 12], and $Ba_8Y_6Ge_{40}$ (Y = Cu, Ni) [13–15]. The $Ba_8Ga_{16}Ge_{30}$ system was recently shown to have partially ordered host structure, where the order depends on the synthesis conditions [16]. Investigations of $Ba_8Al_{16}Ge_{30}$ have revealed that the actual position of the guest atom is largely influenced by the specific positions of the host structure atoms [17]. The 6c site can accommodate larger atoms than 16i and 24k, and therefore Cu and Ni preferentially occupy this site in $Ba_8Cu_6Ge_{40}$ and $Ba_8Ni_6Ge_{40}$ [13–15]. In the case of $Ba_8Zn_8Ge_{38}$, six of the eight Zn can occupy the 6c site, but at least two Zn atoms must occupy other sites.

Here we present neutron diffraction data of $Ba_8Zn_8Ge_{38}$ measured at 20 and 300 K on two differently prepared samples. Neutron diffraction provides larger contrast between Zn and Ge than x-ray diffraction, as the scattering lengths are 5.68 and 8.19 fm, respectively. Additionally, transport properties have been measured in the temperature range from 2 to 400 K on a large single crystal of $Ba_8Zn_8Ge_{38}$ from the slow cooled synthesis batch.

2. Experimental details

2.1. Synthesis

Both samples were prepared using a Zn self-flux method with stoichiometric amounts of the elements Ba:Zn:Ge (8:8:38) plus an additional 50 wt% of Zn as flux media. Both samples were heated above the melting temperature of Ge and allowed to cool to room temperature. Two different samples were obtained by varying the cooling rate (10 and 2 °C h^{-1}). The samples will be referred to as $Ba_8Zn_8Ge_{38}$ fast cooled (FC) and $Ba_8Zn_8Ge_{38}$ slow cooled (SC). After heat treatment the samples were soaked in HCl for 24 h to remove excess flux. The products were reflective shining crystals with clear facets.

2.2. Transport properties

A single crystal from the slow cooled batch was selected for measurements of transport properties. The sample was cut into a rectangular shape with dimensions 2 × 2 × 5 mm^3 and 4-wires were mounted using silver-epoxy. Simultaneous measurements of resistivity, Seebeck coefficient and thermal conductivity were carried out in continues mode using the thermal transport option (TTO) of a Quantum Design, Physical Property Measure Systems (PPMS) [18]. Data was measured in the temperature range from 2 to 400 K.

Table 1. Crystallographic information for the fast cooled (FC) and the slow cooled (SC) $Ba_8Zn_8Ge_{38}$ samples.

20 K	$Ba_8Zn_8Ge_{38}$ FC	$Ba_8Zn_8Ge_{38}$ SC
Space group	$Pm\bar{3}n$	$Pm\bar{3}n$
a (Å)	10.719(1)	10.716(1)
ρ^{calc} (g cm^{-3})	5.91	5.91
Crystal mass (mg)	29.7	167
# Int. refs.	16 136	20 475
# Unique refs.	4851	11 506
$\sin(\theta)/\lambda_{max}$ ($Å^{-1}$)	1.6	1.6
R_F ($F > 3\sigma(F)$) (Ba6d)	15.6%	15.4%
R_F ($F > 3\sigma(F)$) (Ba24j)	15.6%	15.5%
R_F ($F > 3\sigma(F)$) (Ba24k)	15.6%	15.4%

2.3. Single crystal neutron diffraction

The time-of-flight Laue single crystal diffractometer SCD, at the Intense Pulsed Neutron Source (IPNS), Argonne National Laboratory, was used for the single crystal neutron diffraction measurements [19]. A crystal from each synthesis batch was selected and data were measured at 20 and 300 K. Table 1 gives selected crystallographic information. The data were integrated using the ISAW software and absorptions corrections were done with the program ANVRED [20–22]. Structural refinements were carried out using GSAS [23]. Three different models were used in the refinement of the barium guest atom in the large cage, and the models will be referred to as Ba6d (center position with anisotropic atomic displacement parameters (ADPs)), Ba24j (Ba at $(1/4, y, 1/2+y)$ with an isotropic ADP) and Ba24k (Ba at $(1/4 + x, 1/2, z)$ with an isotropic APD). In all models the host structure sites were constrained to be fully occupied, and a chemical constraint was imposed to keep the stoichiometry at $Ba_8Zn_8Ge_{38}$.

3. Results and discussion

3.1. Transport properties

The resistivity data reveal that the SC sample has a semiconducting behavior with a fairly high resistivity (∼500 mΩ cm at 400 K). The resistivity is shown in figure 2 along with the Seebeck coefficient. The negative Seebeck coefficient shows that the majority of charge carriers are electrons making the SC sample an n-type conductor. The synthesis conditions in the present study are similar to those used to obtain p-type $Ba_8Ga_{16}Ge_{30}$, and therefore a p-type conductor may have been expected [16]. The absolute value of the Seebeck coefficient is high, $S = -175\ \mu V\ K^{-1}$ at 400 K, but the high resistivity results in a low power factor ($S^2\sigma$), and thus the corresponding zT value is too low for the SC sample to be good a thermoelectric material. The thermal conductivity is $\kappa_L = 1.4\ W\ K^{-1}\ m^{-1}$ around 250 K (see figure 3). The electronic contribution to the

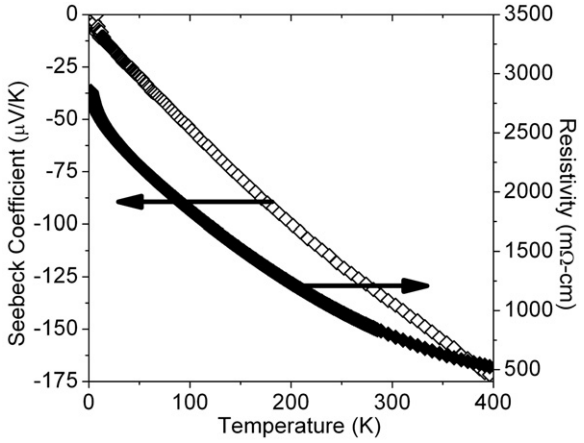

Figure 2. The Seebeck coefficient and resistivity of the slow cooled sample.

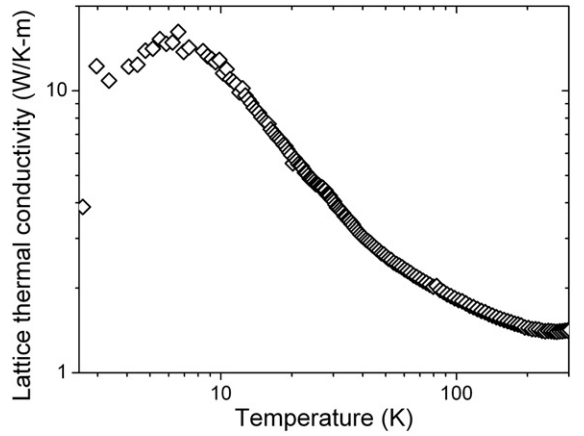

Figure 3. The thermal conductivity of the slow cooled sample.

thermal conductivity is essentially negligible due to the high resistivity. From the semiconducting properties of the SC $Ba_8Zn_8Ge_{38}$ sample it can be concluded, that the stoichiometry is in agreement with the Zintl concept. The resistivity potentially can be reduced by doping to make $Ba_8Zn_8Ge_{38}$ a better thermoelectric material. The reported resistivity for $Ba_8Zn_{7.7}Ge_{38.3}$ is more than 500 times smaller than the resistivity observed for the SC $Ba_8Zn_8Ge_{38}$ sample [6]. The Seebeck coefficient for $Ba_8Zn_{7.7}Ge_{38.3}$ reaches about -100 μV K^{-1} at 400 K [6]. The comparison reveals that the physical properties are very sensitive to minor variations in the Zn content, since the difference is only 0.65% of the total 46 host structure atoms. For comparison the reported thermal conductivity at 200 K is about 2.0 W K^{-1} m^{-1} for $Ba_8Zn_{7.7}Ge_{38.3}$, 1.4 W K^{-1} m^{-1} for n-type $Ba_8Ga_{16}Ge_{30}$, and 2.5 W K^{-1} m^{-1} for $Ba_8Cu_6Ge_{40}$ [6, 13, 24]. However, direct comparison is somewhat difficult since the samples were synthesized with different methods. Thus, n-type $Ba_8Ga_{16}Ge_{30}$ was cut from a single crystal [24], $Ba_8Cu_6Ge_{40}$ was pressed from powder [13], while the preparation method for the $Ba_8Zn_{7.7}Ge_{38.3}$ sample used for transport measurements was not reported [6]. However, additional grain boundary scattering in the case of pressed powder in $Ba_8Cu_6Ge_{40}$ would

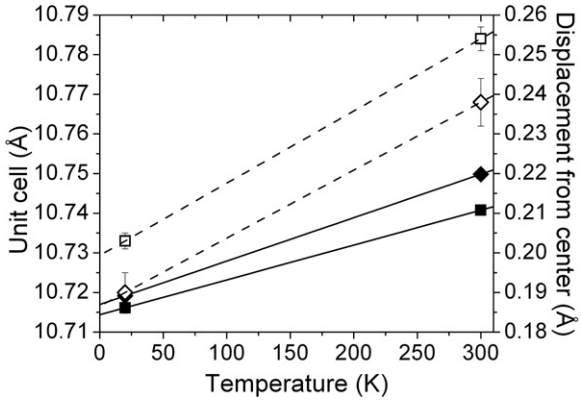

Figure 4. The unit cell (solid symbols) and barium displacement from the center of the cage (open symbols). The slow cooled sample has squares and the fast cooled sample has diamonds. The lines represent a linear model.

be expected to lead to a lower thermal conductivity compared to $Ba_8Zn_8Ge_{38}$, whereas the opposite trend is in fact observed. The mass difference associated with the neighboring elements Cu, Zn, Ga and Ge is fairly small and unlikely to cause the large difference observed. The difference is more likely to be associated with the coupling between the host structure and the barium guest atom. In the case of $Ba_8Al_{16}Ge_{30}$ the thermal conductivity was found to differ by a factor of 3 between two compounds with varying degree of guest atom and host structure order [17].

3.2. Single crystal neutron diffraction

The modeling of the single crystal neutron diffraction data provides information about the host structure occupancy, the guest atom siting, and the Einstein and Debye temperatures. The relevant information has been extracted from the refinement results, and the results are described below. Full information about the refinements is tabulated in the supplementary material. The different structural models have very similar reliability values (R-values), and the nuclear density of the barium guest atom therefore can be described either by an on-center atom with an anisotropic ADP, or an off-center atom with isotropic ADPs.

3.2.1. Barium guest atom siting. The Ba24j and Ba24k models have been used to describe the off-center nuclear density of the barium guest atom in the large cage. Figure 4 shows the unit cell expansion and the distance between the cage center and the Ba atom in the Ba24k model for the SC and FC samples. The distance was found to be identical within the uncertainty for the Ba24j and the Ba24k model. The barium guest atom displacement from the center increases faster than the unit cell expansion for both the SC and the FC sample. The SC sample has a larger displacement from the center than the FC sample, but the temperature dependence of the displacement appears to be identical for the two samples.

The nuclear density around the center of the large cage is shown in figure 5. The nuclear density has been extracted

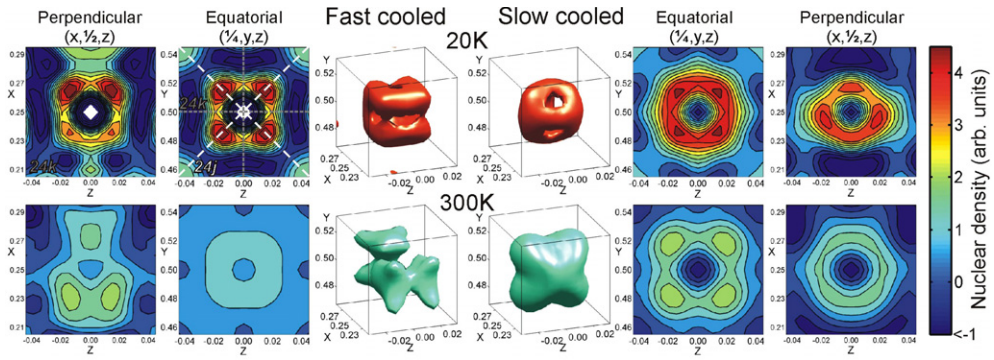

Figure 5. The nuclear density in the large cage extracted from a Fourier difference map with the barium guest atom removed from the model. The left-hand side shows the fast cooled sample, whereas right-hand side shows the slow cooled sample. The upper figures correspond to data measured at 20 K, and the lower figures correspond to 300 K. The center shows isosurface plots, whereas the other figures are contour plots in the equatorial and perpendicular planes. All plots are centered at (1/4, 1/2, 0). The 24k position can be anywhere in the first upper left plot and the dashed lines in the second upper left plots shows the 24j (white) and 24k (gray) positions.

from a Fourier difference map calculated with the Ba2 guest atom removed from the model. At 20 K the FC sample reveals local maxima in the nuclear density at both the 24j and the 24k positions. At 300 K the maxima have shifted towards the 24k positions. The isosurface goes from an approximate hollow box at 20 K to two separated density regions at 300 K. The SC sample is also observed to have local maxima in the nuclear density at the 24j position and 20 K. Weaker maxima are observed in the 24k plane. At 300 K local maxima are observed at 24j, whereas a ring of equal density is observed in the 24k plane. The isosurface reveals a hollow sphere, which is almost unaltered with temperature. The SC sample appears to have a significantly higher density at the 24j position at 300 K compared with the FC sample.

The recent study by Melnychenko-Koblyuk *et al* reports the barium guest atom to be centered, and no off-center modeling was performed [6]. The sample in that study was prepared by quenching and annealing. The different preparation method may explain the different results. Moreover the samples were only investigated with single crystal x-ray diffraction and powder neutron diffraction. These methods are inferior to single crystal neutron diffraction when studying fine features of the nuclear density. Recent studies of $Ba_8Ga_{16}Ge_{30}$ and $Ba_8Al_{16}Ge_{30}$ revealed that the shape of the nuclear density is sensitive to the position of the group 13 element in the host structure. The $Ba_8Ga_{16}Ge_{30}$ samples revealed a change from the 24j positions at ∼20 K to 24k and 6d positions at elevated temperatures (300 K) [16]. In $Ba_8Al_{16}Ge_{30}$ the nuclear density at 20 K depends on the Al occupancy in the host structure. A sample with almost full Al occupancy at the 6c site had the Ba nuclear density concentrated in the perpendicular plane, whereas a sample with ∼55% Al occupancy at the 6c site had the nuclear density confined to the equatorial plane [17]. The results observed for the two $Ba_8Zn_8Ge_{38}$ samples appear to be a mixture of the extreme cases observed for $Ba_8Al_{16}Ge_{30}$.

3.2.2. Einstein and Debye temperature. The ADPs extracted from the Ba6d model are shown in figure 6 along with Einstein and Debye models. The largest ADPs are for both samples

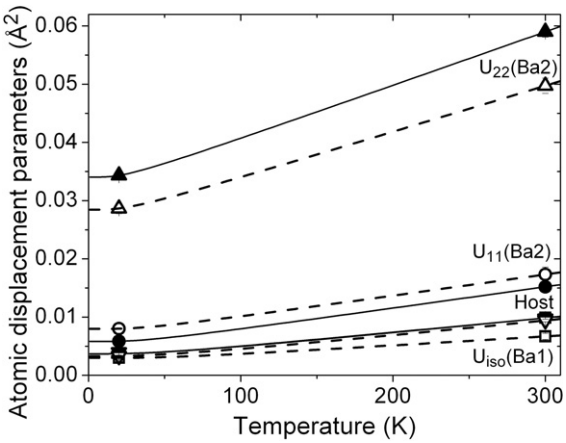

Figure 6. The atomic displacement parameters for the fast cooled (open) and slow cooled (solid) samples. The different atoms have different symbols; U_{22}(Ba2) (triangles pointing up), U_{11}(Ba2) (circles), U_{iso}(Ba1) (squares), and the averaged U_{iso}(host) (triangles pointing down). U_{iso}(host) for both samples and U_{iso}(Ba1) for the slow cooled sample are identical within uncertainties, and consequently they are indistinguishable in the figure. The lines represent Einstein and Debye models of the barium guest atoms and the host structure atoms, respectively. For the fast cooled sample dashed lines have been used, whereas the slow cooled sample is shown with solid lines.

U_{22}(Ba2) followed by the U_{11}(Ba2). The host structure ADPs and U_{iso}(Ba1) are approximately equal. The SC sample has significantly higher U_{22}(Ba2) values than the FC sample, whereas the opposite trend is observed for U_{11} (Ba2). The host structure APDs appear to be almost identical for the SC and FC samples.

Einstein temperature. The guest atom ADPs can be modeled with the Einstein expression (table 2).

$$U_{xx}(T) = \frac{\hbar^2}{2mk_B\theta_{E,xx}} \coth\left(\frac{\theta_{E,xx}}{2T}\right) + d_{xx}^2.$$

The subscripts xx refer to the vibrational direction, m is the Ba mass, $\theta_{E,xx}$ is the Einstein temperature and d_{xx}^2 is a

Table 2. Einstein and Debye temperatures obtained from the refined ADPs.

	U_{iso} (Ba1)	U_{11} (Ba2)	U_{22} (Ba2)	U_{iso} (host)
$\theta_{E,xx}/\theta_D$ (SC)	118	98	62	279
$\theta_{E,xx}/\theta_D$ (FC)	149	98	67	280
d_{xx} (SC)	0.047	0.063	0.177	0.043
d_{xx} (FC)	0.043	0.079	0.161	0.038

temperature independent disorder term. Since data only are available at two temperatures, the number of parameters equals the number of observations. This means that uncertainties cannot be estimated for the model parameters, although they are likely to be similar to the esds obtained in our previous studies using the same type of analysis [16, 17]. For both the $Ba_8Zn_8Ge_{38}$ samples $\theta_{E,22}$(Ba2) is the lowest Einstein temperature and $\theta_{E,iso}$(Ba1) the largest. The temperature independent disorder d_{xx} decreases from d_{22}(Ba2) to d_{11}(Ba2), and d_{iso}(Ba1). The FC sample has a slightly larger $\theta_{E,22}$(Ba2) and also a significantly larger $\theta_{E,iso}$(Ba1). The SC sample has the largest d_{22}(Ba2) disorder, whereas d_{11}(Ba2) is largest for FC. The larger d_{22}(Ba2) of the SC sample is in agreement with the Ba atom being farther from the cage center in the Ba24k and Ba24j models (see figure 4), and the larger disorder in the equatorial plane also agrees with the nuclear density at 300 K in figure 5. The larger d_{11}(Ba2) disorder for the FC sample also agrees with the nuclear density plots. The Einstein temperature compares well with other studies, where $\theta_{E,22}$(Ba2) for $Ba_8Zn_{7.7}Ge_{38.3}$ is 64 K [6], 67 K for $Ba_8Al_{16}Ge_{30}$ and 60 K for $Ba_8Ga_{16}Ge_{30}$ [16, 17]. The Einstein temperature for the Ba2 perpendicular direction and the barium in the small cage likewise compare well between the different compounds, and the disorder values, d_{xx}, are also comparable to the values obtained for $Ba_8Al_{16}Ge_{30}$ and $Ba_8Ga_{16}Ge_{30}$ [16, 17].

Debye temperature. The averaged ADPs of the host structure can be modeled with the Debye expression,

$$U_{iso}(T) = \frac{3\hbar^2 T}{m k_B \theta_D^2}\left[\frac{T}{\theta_D}\int_0^{\theta_D/T}\frac{x}{\exp(x)-1}\,dx + \frac{\theta_D}{4T}\right] + d^2,$$

where m is the average mass of Zn and Ge, θ_D is the Debye temperature and d^2 describes the temperature independent disorder. The last column in table 2 gives the Debye temperature and associated disorder parameter. The Debye temperature is found to be 279 and 280 K, with disorder parameters of 0.043 and 0.038 Å for the SC and FC samples, respectively. In other words the dynamics of the host structures appear to be similar in the two cases. The Debye temperatures compares well with the Debye temperatures found for $Ba_8Al_{16}Ge_{30}$ (∼290 K) and $Ba_8Ga_{16}Ge_{30}$ (∼270 K) [16, 17]. As expected, the heavier host structure atoms lead to lower Debye temperatures. In a first approximation the lattice thermal conductivity is proportional to the Debye temperature, and therefore the lattice thermal conductivity is expected to be fairly identical for the three clathrate type I structures; $Ba_8Zn_8Ge_{38}$, $Ba_8Al_{16}Ge_{30}$, and $Ba_8Ga_{16}Ge_{30}$. The Debye temperature extracted from ADPs for $Sr_8Zn_8Ge_{38}$ was found to be 270 K [12]. Melnychenko-Koblyuk *et al* did not report the Debye temperature for $Ba_8Zn_{7.7}Ge_{38}$, obtained from ADPs, however the Debye temperature obtained from the heat capacity was reported to be 225 or 240 K depending on the model [6].

Table 3. Refined Zn occupancies for the slow cooled (SC) and fast cooled (FC) samples.

Zn%	6c	16i	24k
SC	84(1)	8(1)	7(1)
FC	84(1)	1(2)	12(1)

3.2.3. Host structure occupancy. The enhanced contrast obtained with neutron diffraction compared with x-ray diffraction allows refinement of the host structure occupancy of the next neighboring elements Zn and Ge. The results from the refinements at 20 K are shown in table 3. The occupancy refined from the 300 K data match within uncertainties the values found at 20 K. In both cases the 6c site clearly holds the majority of the Zn (84(1)%). The SC sample has similar Zn occupancies on the 16i and 24k sites (8(1)% and 7(1)%). The FC sample appears to be void of Zn on the 16i site with a refined occupancy of 1(2)%. The 24k site has a Zn occupancy of 12(1)%. From the refinements it can be deduced that the 6c site is not fully occupied by Zn and depending on the synthesis conditions Zn enters the 16i and 24k sites.

The differences in occupancies are relative small. However, the 8% Zn on the 16i site is important as it corresponds to one Zn atom in the equatorial plane in about 2/3 of all large cages. The 16i site is closer to the center of the cage than the 24k site in the equatorial plane. Therefore, Zn atoms at the 16i site will have a larger influence on the guest atom, than Zn at the 24k site. The Zn atom at the 16i site can be expected to cause a perturbation of the potential surface in the large cage. Since diffraction is a time and space averaged probe, the following two scenarios can not distinguished; (1) the Zn atom, needing two electrons to fulfill tetrahedral bonding, attracts the barium guest atom towards the cage wall, or (2) the large volume of Zn compared to Ge pushes the barium away from the 16i site towards the opposite cage wall. Local probes like NMR or EXAFS may shed more light on this issue. In either case Zn will cause a perturbation, which potentially can be observed in the nuclear density. Theoretical calculations support that there is significant host–guest interactions in $X_8Ga_{16}Ge_{30}$ (X = Sr, Ba) [25]. The SC sample with 8(1)% Zn at the 16i site has a larger nuclear density in the equatorial plane of the large cage compared with the FC sample, and this difference may be explained by the perturbation caused by Zn atoms in the equatorial plane.

Correlation between synthesis conditions and host structure occupancies was also demonstrated for $Ba_8Ga_{16}Ge_{30}$, $Ba_8Al_{16}Ge_{30}$, and $Ba_8Ga_{16}Si_{30}$ [16, 17, 26]. In $Ba_8Ga_{16}Ge_{30}$ and $Ba_8Ga_{16}Si_{30}$ it appears that the Ga atoms avoid the 16i site with Ga occupancies around 17% and 8%, respectively. For $Ba_8Al_{16}Ge_{30}$ larger variations were observed on the 16i site (24–43%). In case of $Ba_8Al_{16}Ge_{30}$ a clear correlation between Al occupancy and Ba nuclear density could be deduced,

whereas for $Ba_8Ga_{16}Ge_{30}$ the effect was more subtle. The $Ba_8Zn_{7.7}Ge_{38.3}$ sample was reported to have full Zn occupancy at the 6c site, a partial Zn occupancy at the 16i site, and no Zn on the 24k site [6]. The observed differences in occupancies may be explained with the summation rules proposed by Christensen *et al* [17]. The summation rules were originally proposed for trivalent elements and the summed occupancy of low valence host atoms on 6c and 24k sites should not exceed 100%. Full occupancy at the 6c site therefore forces the Zn atoms to occupy the 16i site. The related compound $Sr_8Zn_8Ge_{38}$ had 88% Zn on the 6c site, 10% Zn on the 16i site, and a 24k site void of Zn [12].

4. Conclusion

Two different samples of $Ba_8Zn_8Ge_{38}$ have been prepared by a self-flux method. Transport properties reveal the slow cooled sample to be a semiconductor. Single crystal neutron diffraction reveals distinct differences in the nuclear density of the barium guest atom in the large cage. The difference in nuclear density was supported by disorder parameters extracted from the atomic displacement parameters with an Einstein oscillator model. Structural modeling with the Ba atom at an off-center position confirms that the barium guest atom is displaced further from the cage center in the slow cooled sample compared with the fast cooled sample. The behavior of the barium guest atom correlates with the refined Zn occupancies. The slow cooled sample has Zn at the 16i site, which corresponds to 2/3 of all cages having a Zn atom in the equatorial plane. These Zn atoms perturb the cage potential and influence the barium guest atom dynamics.

Acknowledgments

The authors are grateful for the neutron beam time obtained at the SCD at the Intense Pulsed Neutron Source, Argonne National Laboratory. Assistance during the measurements by M Miller and A Schultz is highly appreciated. The work was supported by DANSCATT.

References

[1] Fujita I, Kishimoto K, Sato M, Anno H and Koyanagi T 2006 *J. Appl. Phys.* **99** 093707
[2] Paschen S, Carrillo-Cabrera W, Bentien A, Tran V H, Baenitz M, Grin Y and Steglich F 2001 *Phys. Rev.* B **64** 214404
[3] Paschen S, Pacheco V, Bentien A, Sanchez A, Carrillo-Cabrera W, Baenitz M, Iversen B B, Grin Y and Steglich F 2003 *Physica* B **328** 39–43
[4] Bentien A, Pacheco V, Paschen S, Grin Y and Steglich F 2005 *Phys. Rev.* B **71** 165206
[5] Kuhl B, Czybulka A and Schuster H 1995 *Z. Anorg. Allg. Chem.* **621** 1–6
[6] Melnychenko-Koblyuk N, Grytsiv A, Fornasari L, Kaldarar H, Michor H, Rohrbacher F, Koza M, Royanian E, Bauer E, Rogl P, Rotter M, Schmid H, Marabelli F, Devishvili A, Doerr M and Giester G 2007 *J. Phys.: Condens. Matter* **19** 216223
[7] Nolas G S, Cohn J L, Slack G A and Schujman S B 1998 *Appl. Phys. Lett.* **73** 3133–44
[8] Sales B C, Chakoumakos B C, Jin R, Thompson J R and Mandrus D 2001 *Phys. Rev.* B. **63** 245113
[9] Bentien A, Palmqvist A E C, Bryan J D, Latturner S, Stucky G D, Furenlid L and Iversen B B 2000 *Angew. Chem. Int. Edn* **39** 3613–6
[10] Zhang Y G, Lee P L, Nolas G S and Wilkinson A P 2002 *Appl. Phys. Lett.* **80** 2931–3
[11] Bentien A, Nishibori E, Paschen S and Iversen B B 2005 *Phys. Rev.* B **71** 144107
[12] Qiu L, Swainson I P, Nolas G S and White M A 2004 *Phys. Rev.* B **70** 035208
[13] Johnsen S, Bentien A, Madsen G K H, Iversen B B and Nygren M 2006 *Chem. Mater.* **18** 4633–42
[14] Bentien A, Johnsen S and Iversen B B 2006 *Phys. Rev.* B **73** 094301
[15] Johnsen S, Bentien A, Madsen G K H, Nygren M and Iversen B B 2007 at press
[16] Christensen M, Lock N, Overgaard J and Iversen B B 2006 *J. Am. Chem. Soc.* **128** 15657–65
[17] Christensen M and Iversen B B 2007 *Chem. Mater.* **19** 4896–905
[18] Quantum Design 2002 *User's Handbook; Thermal Transport Option (TTO)* 2nd edn, San Diego, CA
[19] Schultz A J 1993 *Trans. Am. Crystallogr. Assoc.* **29** 29–41
[20] Worlton T 2005 v. 1.8.0 alpha5
[21] Schultz A J and Leung P C W 1986 *J. Physique Coll.* C **5** 137–42
[22] Schultz A J 1987 *Trans. Am. Crystallogr. Assoc.* **23** 61–9
[23] Larson A C and Dreele R B V 2004 *Los Alamos National Laboratory Report LAUR 86-748*
[24] Bentien A, Christensen M, Bryan J D, Sanchez A, Paschen S, Steglich F, Stucky G D and Iversen B B 2004 *Phys. Rev.* B **69** 045107
[25] Gatti C, Bertini L, Blake N P and Iversen B B 2003 *Chem. Eur. J.* **9** 4556–68
[26] Christensen M and Iversen B B 2006 *Proc. 4th Eur. Conf. on Thermoelectrics (Cardiff, UK)* ed D M Rowe